International Journal of Solids and Structures 135 (2018) 261–273

Contents lists available at ScienceDirect

International Journal of Solids and Structures

journal homepage: www.elsevier.com/locate/ijsolstr

Insights on the vibration characteristics of double-layer cable nets of D_{4h} symmetry

Alphose Zingoni

Department of Civil Engineering, University of Cape Town, Rondebosch 7701, Cape Town, South Africa

ARTICLE INFO

Article history:
Received 19 July 2017
Revised 9 November 2017
Available online 29 November 2017

Keywords:
Cable net
Vibration
Symmetry
Group theory
Eigenvalue problem
Mode shape

ABSTRACT

Coupling shallow cable nets into multi-layer configurations offers the possibility of altering the vibration properties of single-layer systems in a beneficial way. When members of appropriate stiffness and damping characteristics are employed as coupling devices, there will be a dynamic interaction between the motions of the layers, with the combined system expected to exhibit a higher stiffness and damping response than the individual layers. Vertical coupling of two identical single-layer cable nets of C_{4v} symmetry results in a double-layer configuration of D_{4h} symmetry, the vertical motions of which are strongly influenced by the symmetry properties of the configuration as well as the stiffness and damping properties of the coupling members. By considering a 32-node double-layer cable net as a case study, the present investigation employs group theory to reveal important insights on the vibration characteristics of cable nets of the type in question, at the same time laying out a computational framework for an efficient vibration analysis of such systems.

1. Introduction

Cable nets find application as lightweight roofing systems for long spans (Otto, 1966; Irvine, 1981; Szabo and Kollar, 1984; Vilnay, 1990). They may be formed by prestressing a set of cables running in one direction against another set of cables running in the perpendicular direction, with the two systems of cables being curved in opposite directions. The result is an orthogonal net capable of resisting external loads, and the stiffness of this structure is very much a function of the tensile forces in the individual cables. In other arrangements, three or more cable systems may be employed, with these being inclined at angles other than 90°.

In many roofing applications, cable nets are usually shallow, with the vertical rise (or fall) of the net being relatively small in comparison with the lateral dimensions of the net. For present purposes, cable nets may be considered as shallow if the rise-to-span ratio is less than 1/5. For such shallow nets, the reference plane for transverse motions may be taken as horizontal, an approach similar to the approximation often adopted in the static analysis of shallow shells (Zingoni, 1997). In the present investigation, we will be interested only in the small transverse motions (i.e. vertical vibrations) of shallow cable nets, where one set of cables is assumed to run in the x coordinate direction and the other set of cables is assumed to run in the y coordinate direction, with the transverse direction being vertical and denoted by the z axis.

The motion of the cable net will be represented by discrete masses located at the intersections of the cables, and the cables will be assumed to have tensile stiffness but no mass. In the modelling of the physical system, all the mass of the cables (and any additional mass contributed by roof cladding and other fittings) is lumped at the nodes of the cable net. Lumped-parameter modelling is not as exact as distributed-parameter modelling, but for the purposes of gaining important insights on the key features of the vibration response of the system, it is adequate. Unlike distributed-parameter modelling which results in partial differential equations of motion, lumped-parameter modelling results in ordinary differential equations which are simpler to solve (Zingoni, 2015).

Other assumptions that we will make are that the tensions in the cables are relatively large, and the transverse displacements of the cable net remain relatively small during vibration, so that the magnitudes of the tensile forces in the cables do not change appreciably during the motion. Moreover, the friction between the cables at their intersections is considered to be negligible, so that the tensile force in a given cable remains practically constant throughout its length. These assumptions can be realised to a very good degree in many practical situations.

The dynamic behaviour of cable nets has been the subject of numerous investigations. While the response of cable nets to static loads and time-varying excitations is generally characterised by geometric non-linearities (Siev, 1963; Buchholdt et al., 1968; Ivovich and Pokrovskii, 1991), essentially linear techniques may

E-mail address: alphose.zingoni@uct.ac.za

https://doi.org/10.1016/j.ijsolstr.2017.11.025
0020-7683/

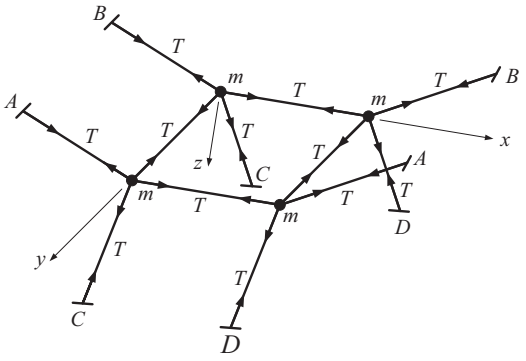

Fig. 1. A single-layer cable net with four nodes and C_{4v} symmetry.

be used to investigate their behaviour, provided the displacements are not too large (Calladine, 1982; Pellegrino and Calladine, 1984; Vilnay and Rogers, 1990).

For reasons to do with function and aesthetics, many cable nets possess one or more symmetry properties. The symmetry properties of a structure have a distinct influence upon the static and kinematic behaviour of the structure (Zingoni et al., 1995a, 1995b; Kangwai et al., 1999; Kangwai and Guest, 1999, 2000; Fowler and Guest, 2000; Guest and Fowler, 2007; Chen et al., 2015a), and special methods employed to analyse this behaviour include those based on graph theory and its variants (Kaveh and Rahami, 2004; Kaveh and Nikbakht, 2007, 2010; Kaveh and Koohestani, 2008; Chen and Feng, 2016), and those based on group theory (Healey, 1988; Zlokovic, 1989; Ikeda and Murota, 1991; Healey and Treacy, 1991; Mohan and Pratap, 2004; Zingoni, 1996, 2005, 2008, 2012a; Chen and Feng, 2012; Harth and Michelberger, 2016). Group theory is particularly suited to the study of physical systems possessing complex symmetry properties, and its applications in various areas of physics and chemistry are well known (Weyl, 1932; Wigner, 1959; Hamermesh, 1962; Schonland, 1965). Within structural mechanics, the approach leads to considerable reductions in computational effort in problems of the vibration, stability and bifurcation of structures (Zingoni, 2009), and also affords valuable insights on structural behaviour (Zingoni, 2014; Chen et al., 2015b). Since symmetry is not always easy to identify (particularly in complex structures), a significant amount of effort has also been directed towards developing procedures for the automatic recognition of symmetry (Suresh and Sirpotdar, 2006; Zingoni, 2012b).

In a previous study (Zingoni, 1996), the vibration of single-layer high-tension shallow cable nets with C_{2v} and C_{4v} symmetries in plan (i.e. the symmetries of a rectangle and a square, respectively) were considered. Through use of group theory, vibration modes having coincident frequencies were identified, and other predictions (such as the existence of stationary nodes and nodal lines) were made. In the present work, we employ group theory to study the vibration characteristics of double-layer cable nets belonging to the symmetry group D_{4h}. Such cable nets are formed when two single-layer cable nets of C_{4v} symmetry are coupled in the vertical direction. The higher-order symmetry of D_{4h} cable nets complicates their vibration response, and group theory becomes particularly useful for unravelling the complexities and fully understanding the dynamic response.

Fig. 1 shows a very simple single-layer cable net comprising two cables *AA* and *BB* in vertical planes parallel to the *xz* plane, crossed by two cables *CC* and *DD* in vertical planes parallel to the *yz* plane, the whole arrangement having the symmetry of a square (i.e. C_{4v} symmetry) in plan. Each cable carries a tensile force of magnitude *T*. Equal masses of magnitude *m* are assumed at each of the four cable intersections. The self-stressing system has four degrees of freedom comprising the vertical motions of each of these masses.

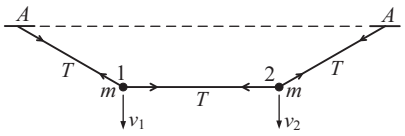

Fig. 2. Vertical section in the plane of cable *AA* of the single-layer cable net with four nodes. The vertical degrees of freedom of the masses at nodes 1 and 2 are v_1 and v_2.

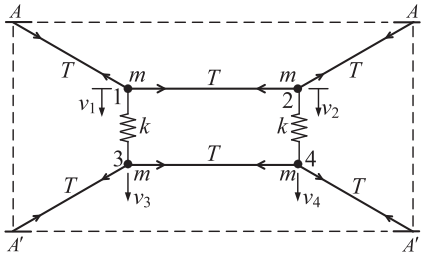

Fig. 3. Vertical coupling of two identical single-layer cable nets of C_{4v} symmetry to form a double-layer cable net of D_{4h} symmetry. The coupling is illustrated in the vertical plane of cable *AA* of Fig. 1 (cable *A′A′* being its mirror image in a horizontal plane of symmetry). The connecting devices are modelled as linear springs of stiffness *k*. The vertical degrees of freedom of the masses at nodes {1, 2, 3, 4} are $\{v_1, v_2, v_3, v_4\}$.

Fig. 2 shows the cable net in the vertical plane of cable *AA*, with v_1 and v_2 being the vertical degrees of freedom of the masses at nodes 1 and 2. When two identical single-layer cable nets of C_{4v} symmetry are vertically connected via identical springs, we obtain a double-layer cable net of D_{4h} symmetry. Such coupling is illustrated in Fig. 3, which shows cable *AA* connected to its mirror-image counterpart *A′A′* via coupling devices of spring stiffness *k*. The nodes in this coupling plane are {1, 2, 3, 4}, with associated vertical degrees of freedom being $\{v_1, v_2, v_3, v_4\}$. Similar coupling occurs in the vertical planes of cables *BB*, *CC* and *DD*.

Coupling of shallow cable nets into double-layer configurations offers the possibility of altering the load-carrying and dynamic characteristics of single-layer systems in a beneficial way. Before the benefits of such coupling can be evaluated in a quantitative way, it is useful to gain some insights on the vibration behaviour of double-layer cable nets of D_{4h} symmetry, to get a better understanding of how symmetry influences this behaviour. This is the primary aim of this paper.

Earlier studies have already demonstrated the effectiveness of the group-theoretic formulation in simplifying the analysis of the vibration of plates, single-layer cable nets and layered space grids of C_{nv} symmetry, so in terms of the general approach, the present study is similar. However, the key difference is that the D_{nh} configurations considered in the present paper have rotation and reflection symmetries not only about one central vertical axis and a number of vertical planes passing through this central vertical axis (as with C_{nv} configurations), but they also possess additional rotation symmetries about a number of horizontal axes perpendicular to the central vertical axis, as well as an additional reflection plane that is horizontal (and therefore perpendicular to the central vertical axis). Their symmetry is therefore of higher order, and more complex. Previous studies have mostly focused on simpler C_{nv} configurations.

In terms of vibration behaviour, double-layer cable nets of D_{nh} symmetry exhibit transverse extensional modes (i.e. expansion and contraction of the vertical distance between the two layers) which are irrelevant in the case of single-layer cable nets and other

single-layer structures that have been studied in the past. The spring-like coupling between the two layers permits the upper and lower layers of the cable net to move independently of each other, thus doubling the total number of system degrees of freedom, in comparison with single-layer cable nets (or rigidly connected double-layer cable nets whose layers move up and down together). It is the occurrence of these additional extensional modes (or "breathing" modes) that distinguishes the present study from all the previous ones. Group theory will reveal additional new insights specific to D_{nh} cable-net configurations.

The scope of the present study is limited to cable nets whose configuration fully conforms to the symmetry group D_{nh} in terms of arrangement of members, member properties, pattern of prestressing and support conditions. It should be pointed out that small departures from perfect symmetry (due to, for example, the addition or subtraction of one member, or the inclusion of a member whose properties differ from those of the other members) may also be handled using techniques based on group theory (Varkonyi and Domokos, 2007), or those based on graphs (Kaveh and Shojaei, 2015). Here, we shall not be concerned with imperfect symmetry.

The structure of the rest of the paper is as follows. We will begin by outlining some basic concepts of symmetry and group theory, and describe the properties of symmetry groups D_{2h} and D_{4h}, which are of interest in the present work. This is followed by a description of the double-layer cable net forming the subject of the detailed study. Symmetry-adapted freedoms and basis vectors for the various subspaces of the problem are then derived, and the symmetry properties of these subspaces illustrated by means of basis-vector plots. An analysis of the results is then made, allowing us to gain some insights on the nature of the modes of vibration of the cable net. The results also permit an assessment of the computational benefits of the group-theoretic decomposition to be made. The concluding remarks indicate how the present work will be applied to actual computations.

2. Concepts of symmetry and group theory

A system or an object is said to exhibit symmetry if it can be turned into one or more new configurations physically indistinguishable from the initial configuration through the application of one or more symmetry operations. Symmetry operations include reflections in planes, rotations about axes, or inversions through the centre.

A set of elements $\{\alpha,\ \beta,\ \gamma,\ ...,\ \sigma,\ ...\}$ comprises a *group* G if the following axioms are satisfied:

(i) the product γ of any two elements α and β of the group, which is given by $\gamma=\alpha\beta$, is a unique element which also belongs to the group
(ii) among the elements of G, there is an identity element e which, when multiplied with any element α of the group, leaves the element unchanged: $e\alpha=\alpha e=\alpha$
(iii) each element α of G has an inverse α^{-1} also belonging to the group, such that $\alpha\alpha^{-1}=\alpha^{-1}\alpha=e$
(iv) when three or more elements of G are multiplied, the order of the multiplication does not affect the result: $\alpha(\beta\gamma)=(\alpha\beta)\gamma$

A group where all elements are symmetry operations constitutes a *symmetry group*.

2.1. Symmetry elements of groups D_{2h} and D_{4h}

The symmetry group D_{2h} describes the symmetry of a right prism of rectangular base (Fig. 4(a)). It has the following symmetry elements with respect to the coordinate directions $\{x,\ y,\ z\}$ and associated orthogonal planes $\{xy,\ xz,\ yz\}$:

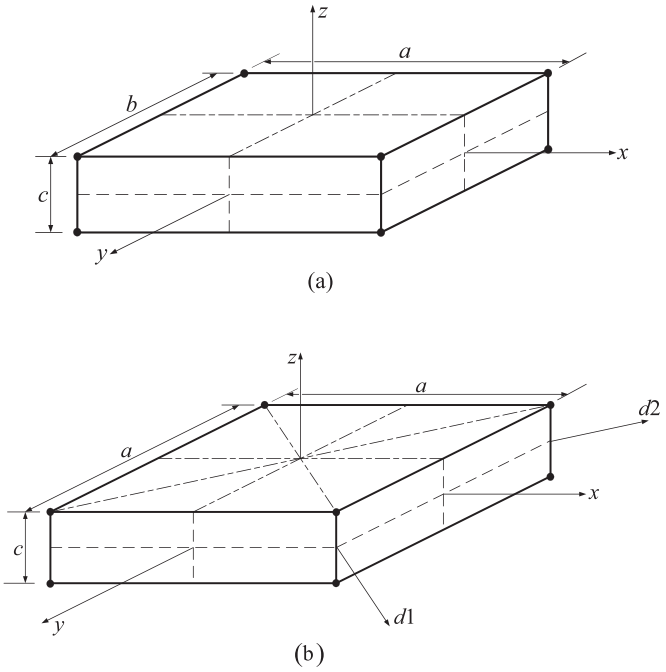

Fig. 4. Symmetry planes and rotation axes of right prisms: (a) D_{2h} prism and (b) D_{4h} prism.

e: identity element
$C_2^z,\ C_2^x, C_2^y$: rotations through an angle of $\pi/2$ about the $\{z,\ x,\ y\}$ axes, respectively
$\sigma_{xy}, \sigma_{xz}, \sigma_{yz}$: reflections in the central $\{xy,\ xz,\ yz\}$ planes, respectively
i: inversion element (reflection through the centre of symmetry of the configuration)

Thus symmetry group D_{2h} is of order 8, the order of a group being the number of symmetry elements making up the group.

The symmetry group D_{4h} describes the symmetry of a right prism of square base (Fig. 4(b)). It has all the eight symmetry elements of group D_{2h}, as well as the following eight additional elements:

$C_4,\ C_4^{-1}$: rotations about the z axis through angles of $\pi/4$ and $-\pi/4$, respectively
$C_2^{d1},\ C_2^{d2}$: rotations through an angle of $\pi/2$ about the two diagonal axes $d1$ and $d2$ (these are perpendicular to each other and at 45° to the x and y axes)
$S_4,\ S_4^{-1}$: rotary-reflections through angles of $\pi/4$ and $-\pi/4$, respectively, these operations consisting of a rotation about the z axis through an angle of $\pi/4$ or $-\pi/4$, followed by a reflection in the central xy plane (note that the inversion element i is equivalent to a rotary-reflection through an angle of $\pi/2$, i.e. equivalent to the operation S_2)
σ_{d1}, σ_{d2}: reflections in the vertical diagonal planes containing the diagonal axes $d1$ and $d2$

Thus the symmetry group D_{4h} is of order 16. In considerations of symmetry groups D_{nh} $(n > 2)$, the central xy plane is usually taken to be horizontal and therefore denoted by the subscript h, with the operation σ_{xy} being denoted by σ_h, and the operations $\{\sigma_{xz}, \sigma_{yz}\}$ being denoted as simply $\{\sigma_x, \sigma_y\}$; the operation C_2^z is simply written as C_2.

Double-layer cable nets may also have symmetries of right prisms based on other regular polygons. The cable-net plan forms

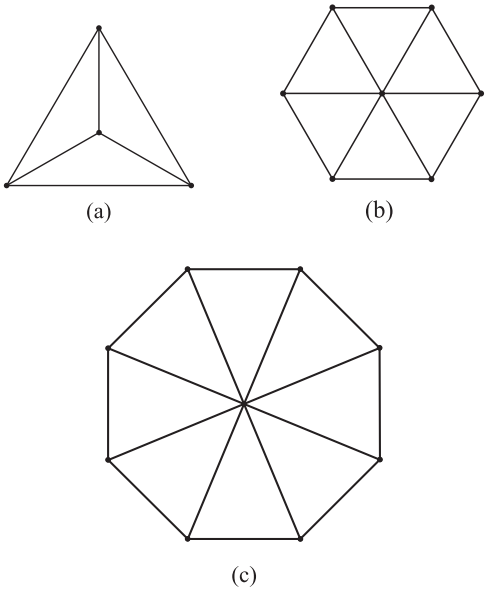

Fig. 5. Plan views of other polygonal prisms: (a) D_{3h} prism; (b) D_{6h} prism and (c) D_{8h} prism.

shown in Fig. 5 are associated with symmetry groups D_{3h}, D_{6h} and D_{8h} of order 12, 24 and 32, respectively.

2.2. Classes of a group

An element α of a group G is said to be conjugate to the element β in the same group if there exists an element ρ in G, such that $\alpha = \rho^{-1}\beta\,\rho$. The collection of all elements formed by evaluating $\rho^{-1}\beta\,\rho$ for all ρ in the group is called the *class* of β. The elements of any finite group can be divided into non-overlapping classes. The class table of a group is constructed by evaluating $\rho^{-1}\beta\,\rho$ for all elements ρ and β of the group, ρ being taken from the left side and β from the top, the product $\rho^{-1}\beta\,\rho$ being entered at the intersection of row ρ and column β. Collecting into a set the distinct elements appearing in each column of the class table, for all columns of the table, gives the classes of the group. The identity element e always belongs to a class of its own.

2.3. Representations of symmetry groups

Let a set of symmetry operators $\{\alpha, \beta, \gamma, ..., \sigma, ...\}$ in an n-dimensional vector space V constitute a group G. The set of matrices describing all the symmetry operators of G, with respect to a particular basis of the n-dimensional vector space, constitutes an n-dimensional representation of G. The trace of a matrix representing an operator σ is called the *character* of σ, denoted by $\chi(\sigma)$. If the basis of V is changed, a new set of matrices, also constituting a representation of the group G, results. Since a basis transformation does not change the trace of a matrix representing a linear operator in an n-dimensional vector space, this second representation of G has the same set of characters as the first representation.

Suppose now that a basis is found with respect to which the matrices of the group representation are expressed as direct sums of submatrices that no further change of basis can reduce to matrices of smaller dimensions. Then sets of these submatrices (a set covering all the symmetry elements of the group) constitute *irreducible representations*. If a group G of order h has k classes, then the number of different irreducible representations is finite and equal to k.

Table 1
Character table of group D_{2h}.

D_{2h}	e	C_2^z	C_2^x	C_2^y	i	σ_{xy}	σ_{xz}	σ_{yz}
A_g	1	1	1	1	1	1	1	1
B_{1g}	1	1	−1	−1	1	1	−1	−1
B_{2g}	1	−1	−1	1	1	−1	1	−1
B_{3g}	1	−1	1	−1	1	−1	−1	1
A_u	1	1	1	1	−1	−1	−1	−1
B_{1u}	1	1	−1	−1	−1	−1	1	1
B_{2u}	1	−1	−1	1	−1	1	−1	1
B_{3u}	1	−1	1	−1	−1	1	1	−1

Table 2
Character table of group D_{4h}.

D_{4h}	e	C_4 C_4^{-1}	C_2	C_2^x C_2^y	C_2^{d1} C_2^{d2}	i	S_4 S_4^{-1}	σ_h	σ_x σ_y	σ_{d1} σ_{d2}
A_{1g}	1	1	1	1	1	1	1	1	1	1
A_{2g}	1	1	1	−1	−1	1	1	1	−1	−1
B_{1g}	1	−1	1	1	−1	1	−1	1	1	−1
B_{2g}	1	−1	1	−1	1	1	−1	1	−1	1
E_g	2	0	−2	0	0	2	0	−2	0	0
A_{1u}	1	1	1	1	1	−1	−1	−1	−1	−1
A_{2u}	1	1	1	−1	−1	−1	−1	−1	1	1
B_{1u}	1	−1	1	1	−1	−1	1	−1	−1	1
B_{2u}	1	−1	1	−1	1	−1	1	−1	1	−1
E_u	2	0	−2	0	0	−2	0	2	0	0

2.4. Character tables

In any irreducible representation, all group elements belonging to the same class have the same character, since traces of conjugate elements are equal. Character tables for the various irreducible representations of common point groups are readily available in the literature (Hamermesh, 1962; Schonland, 1965). Tables 1 and 2 show the character tables of groups D_{2h} and D_{4h} (of interest in the present study).

The rows of the character tables correspond to the various irreducible representations of the group, which are labelled on the extreme left following the usual convention: symbols A and B denote 1-dimensional representations (A indicating symmetry with respect to the principal rotation axis C_n, and B antisymmetry), while E denotes 2-dimensional representations; subscripts g and u denote symmetry and antisymmetry, respectively, with respect to the centre of inversion; subscripts 1 and 2 denote symmetry and antisymmetry, respectively, with respect to a nonprincipal rotation axis (C_2). The sets of characters for different irreducible representations are always different. Any two rows of the character table are orthogonal, as are any two columns. This means that if any two rows are written as algebraic row vectors, their *dot product* is zero, and if any two columns are written as algebraic column vectors, their dot product is also zero.

2.5. Idempotents

The *group algebra* of a group G is the set of all linear combinations of group elements. The group algebra has the properties of a vector space, and the elements of the group G form a basis of the group algebra. The *centre of the group algebra* is the set of all elements that commute with every element of the group algebra. For a given class of the group G as defined earlier, the *class sum* is the sum of all elements belonging to the class. Class sums form a basis of the centre of the group algebra.

Idempotents $P^{(i)}$ of the group algebra are its non-zero elements which satisfy the relation $\{P^{(i)}\}^2 = P^{(i)}$. Orthogonal idempotents satisfy the relation $P^{(i)}P^{(j)} = 0$ if $i \neq j$. They are linearly independent; the sum of orthogonal idempotents is also an idempotent.

Idempotents of the centre of the group algebra are linear combinations of class sums. An idempotent $P^{(i)}$ corresponding to the irreducible representation $R^{(i)}$, by operating on vectors of the space V, nullifies every vector which does not belong to the subspace $S^{(i)}$ of $R^{(i)}$. Thus, out of all the vectors belonging to the group-invariant subspaces $S^{(1)}, S^{(2)}, ..., S^{(k)}$, the operator $P^{(i)}$ selects all vectors belonging to the subspace $S^{(i)}$, and therefore acts as a *projection operator* (Hamermesh, 1962) of the subspace $S^{(i)}$. The orthogonal idempotents of the centre of the group algebra ($P^{(i)}$ for subspace $S^{(i)}$; $i = 1, 2, ..., k$) can be written down directly from the character table using the relation

$$P^{(i)} = \frac{h_i}{h} \sum_{\sigma} \chi_i(\sigma^{-1})\, \sigma \tag{1}$$

where h is the order of G (i.e. the number of elements of G), h_i is the dimension of the ith irreducible representation (given by $h_i = \chi_i(e)$, the first character of the ith row of the character table), χ_i is a character of the ith irreducible representation, σ is an element of G, and σ^{-1} its inverse. The idempotents for groups D_{2h} and D_{4h} are obtained as follows:

Group D_{2h}

$$P^{(1)} = \frac{1}{8}\left(e + C_2^z + C_2^x + C_2^y + i + \sigma_{xy} + \sigma_{xz} + \sigma_{yz}\right) \tag{2a}$$

$$P^{(2)} = \frac{1}{8}\left(e + C_2^z - C_2^x - C_2^y + i + \sigma_{xy} - \sigma_{xz} - \sigma_{yz}\right) \tag{2b}$$

$$P^{(3)} = \frac{1}{8}\left(e - C_2^z - C_2^x + C_2^y + i - \sigma_{xy} + \sigma_{xz} - \sigma_{yz}\right) \tag{2c}$$

$$P^{(4)} = \frac{1}{8}\left(e - C_2^z + C_2^x - C_2^y + i - \sigma_{xy} - \sigma_{xz} + \sigma_{yz}\right) \tag{2d}$$

$$P^{(5)} = \frac{1}{8}\left(e + C_2^z + C_2^x + C_2^y - i - \sigma_{xy} - \sigma_{xz} - \sigma_{yz}\right) \tag{2e}$$

$$P^{(6)} = \frac{1}{8}\left(e + C_2^z - C_2^x - C_2^y - i - \sigma_{xy} + \sigma_{xz} + \sigma_{yz}\right) \tag{2f}$$

$$P^{(7)} = \frac{1}{8}\left(e - C_2^z - C_2^x + C_2^y - i + \sigma_{xy} - \sigma_{xz} + \sigma_{yz}\right) \tag{2g}$$

$$P^{(8)} = \frac{1}{8}\left(e - C_2^z + C_2^x - C_2^y - i + \sigma_{xy} + \sigma_{xz} - \sigma_{yz}\right) \tag{2h}$$

Group D_{4h}

$$P^{(1)} = \frac{1}{16}\left(e + C_4 + C_4^{-1} + C_2 + C_2^x + C_2^y + C_2^{d1} + C_2^{d2} + i + S_4 + S_4^{-1} + \sigma_h + \sigma_x + \sigma_y + \sigma_{d1} + \sigma_{d2}\right) \tag{3a}$$

$$P^{(2)} = \frac{1}{16}\left(e + C_4 + C_4^{-1} + C_2 - C_2^x - C_2^y - C_2^{d1} - C_2^{d2} + i + S_4 + S_4^{-1} + \sigma_h - \sigma_x - \sigma_y - \sigma_{d1} - \sigma_{d2}\right) \tag{3b}$$

$$P^{(3)} = \frac{1}{16}\left(e - C_4 - C_4^{-1} + C_2 + C_2^x + C_2^y - C_2^{d1} - C_2^{d2} + i - S_4 - S_4^{-1} + \sigma_h + \sigma_x + \sigma_y - \sigma_{d1} - \sigma_{d2}\right) \tag{3c}$$

$$P^{(4)} = \frac{1}{16}\left(e - C_4 - C_4^{-1} + C_2 - C_2^x - C_2^y + C_2^{d1} + C_2^{d2} + i - S_4 - S_4^{-1} + \sigma_h - \sigma_x - \sigma_y + \sigma_{d1} + \sigma_{d2}\right) \tag{3d}$$

$$P^{(5)} = \frac{1}{8}(2e - 2C_2 + 2i - 2\sigma_h) = \frac{1}{4}(e - C_2 + i - \sigma_h) \tag{3e}$$

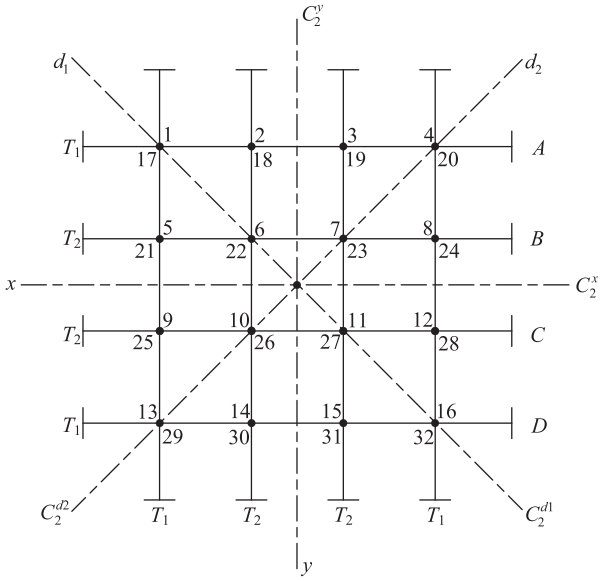

Fig. 6. Plan view of 32-node double-layer cable net of D_{4h} symmetry.

$$P^{(6)} = \frac{1}{16}\left(e + C_4 + C_4^{-1} + C_2 + C_2^x + C_2^y + C_2^{d1} + C_2^{d2} - i - S_4 - S_4^{-1} - \sigma_h - \sigma_x - \sigma_y - \sigma_{d1} - \sigma_{d2}\right) \tag{3f}$$

$$P^{(7)} = \frac{1}{16}\left(e + C_4 + C_4^{-1} + C_2 - C_2^x - C_2^y - C_2^{d1} - C_2^{d2} - i - S_4 - S_4^{-1} - \sigma_h + \sigma_x + \sigma_y + \sigma_{d1} + \sigma_{d2}\right) \tag{3g}$$

$$P^{(8)} = \frac{1}{16}\left(e - C_4 - C_4^{-1} + C_2 + C_2^x + C_2^y - C_2^{d1} - C_2^{d2} - i + S_4 + S_4^{-1} - \sigma_h - \sigma_x - \sigma_y + \sigma_{d1} + \sigma_{d2}\right) \tag{3h}$$

$$P^{(9)} = \frac{1}{16}\left(e - C_4 - C_4^{-1} + C_2 - C_2^x - C_2^y + C_2^{d1} + C_2^{d2} - i + S_4 + S_4^{-1} - \sigma_h + \sigma_x + \sigma_y - \sigma_{d1} - \sigma_{d2}\right) \tag{3i}$$

$$P^{(10)} = \frac{1}{8}(2e - 2C_2 - 2i + 2\sigma_h) = \frac{1}{4}(e - C_2 - i + \sigma_h) \tag{3j}$$

3. A double-layer cable net of D_{4h} symmetry

Fig. 6 shows the horizontal plan view of a 32-node double-layer cable net, with the top-layer nodes numbered 1–16 and the bottom-layer nodes numbered 17–32 as shown. Let us assume that the 3-dimensional cable net (comprising sets of cables of opposed curvature) is very shallow. This allows us to approximate the two layers of cable nodes as flat horizontal planes, as shown in the vertical sections of Fig. 7. The overall configuration belongs to symmetry group D_{4h}.

With reference to the horizontal plan view of Fig. 6, the principal rotation axis C_n is vertical (i.e. perpendicular to the page) and passes through the centre of the diagram; it contains the centre of symmetry of the whole configuration, which is located midway between the two layers of the cable net. The vertical C_n axis is associated with the rotation symmetry operations $\{C_4,\ C_4^{-1},\ C_2\}$. The horizontal reflection plane associated with the symmetry operation σ_h is located at the level of the centre of symmetry of the configuration. The combination of rotations about the C_n axis and reflection

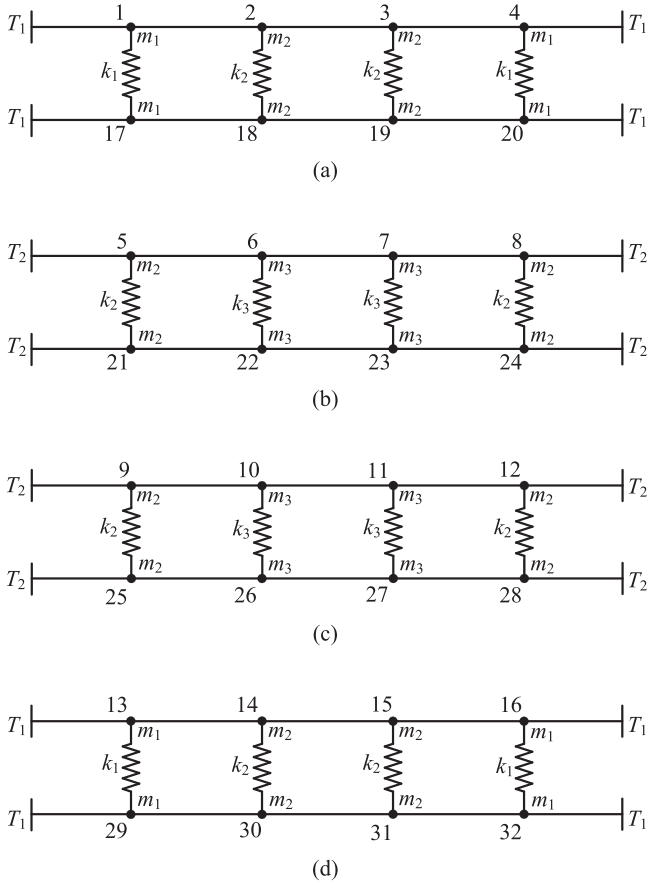

Fig. 7. Vertical sections of the 32-node double-layer cable net (refer to labels in plan view of Fig. 6): (a) section *A*; (b) section *B*; (c) section *C* and (d) section *D*.

in the horizontal central plane gives rise to the rotary-reflection operations $\{S_4,\ S_4^{-1},\ S_2\}$, the last of these being, of course, equivalent to the inversion operation i.

The four vertical reflection planes associated with the symmetry operations $\{\sigma_x, \sigma_y, \sigma_{d1}, \sigma_{d2}\}$ are indicated by the coordinate axes $\{x,\ y\}$ and the diagonal axes $\{d_1, d_2\}$ as shown. These four vertical planes also contain the nonprincipal C_2 rotation axes $\{C_2^x,\ C_2^y,\ C_2^{d1},\ C_2^{d2}\}$ which are all horizontal and pass through the centre of symmetry.

The cables are assumed to carry prestressing forces of magnitude T_1 or T_2. In plan, the arrangement of cable forces conform to C_{4v} symmetry (as is clear from Fig. 6). In elevation, pairs of cables lying in the same vertical plane have the same prestress force (see Fig. 7). Thus the overall pattern of prestressing also conforms to the D_{4h} symmetry of the structural configuration.

The symmetry operations of group D_{4h}, when applied on the nodal positions 1–32 of the double-layer cable net, yield three permutation sets: corner nodes {1, 4, 13, 16, 17, 20, 29, 32}, mid-side nodes {2, 3, 5, 8, 9, 12, 14, 15, 18, 19, 21, 24, 25, 28, 30, 31}, and centre nodes {6, 7, 10, 11, 22, 23, 26, 27}. Consistent with the requirements of D_{4h} symmetry, each node of a given permutation set will be modelled with the same mass, and the vertical members coupling the nodes of a given permutation set will also be assigned the same stiffness. The masses and coupling stiffnesses for the three sets of nodes are denoted by $\{m_1, m_2, m_3\}$ and $\{k_1, k_2, k_3\}$, respectively, as illustrated in Fig. 7.

4. Symmetry-adapted freedoms and subspace basis vectors

To generate the symmetry-adapted freedoms of the first subspace of the problem, we apply the first idempotent of the symmetry group D_{4h} to each of the 32 degrees of freedom of the cable net comprising the vertical motions of the 16 nodes of the top layer and the 16 nodes of the bottom layer (i.e. $v_i\,(i=1,\ 2,\ ...,\ 32)$). Using the expression for $P^{(1)}$as given by Eq. (3a), and applying its symmetry operations on each freedom $v_i\,(i=1,\ 2,\ ...,\ 32)$ in turn, we obtain 32 symmetry-adapted freedoms (many of which are equal to each other) as follows:

$$\begin{aligned}
P^{(1)}v_1 &= \frac{1}{16}\left(e + C_4 + C_4^{-1} + C_2 + C_2^x + C_2^y + C_2^{d1} + C_2^{d2} + i + S_4 \right.\\
&\quad \left. + S_4^{-1} + \sigma_h + \sigma_x + \sigma_y + \sigma_{d1} + \sigma_{d2}\right) v_1\\
&= \frac{1}{16}(v_1 + v_4 + v_{13} + v_{16} + v_{29} + v_{20} + v_{17} + v_{32} + v_{32}\\
&\quad + v_{20} + v_{29} + v_{17} + v_{13} + v_4 + v_1 + v_{16})\\
&= \frac{2}{16}(v_1 + v_4 + v_{13} + v_{16} + v_{17} + v_{20} + v_{29} + v_{32})\\
&= P^{(1)}v_4 = P^{(1)}v_{13} = P^{(1)}v_{16} = P^{(1)}v_{17} = P^{(1)}v_{20}\\
&= P^{(1)}v_{29} = P^{(1)}v_{32}
\end{aligned} \tag{4a}$$

$$\begin{aligned}
P^{(1)}v_2 &= \frac{1}{16}\left(e + C_4 + C_4^{-1} + C_2 + C_2^x + C_2^y + C_2^{d1} + C_2^{d2} + i + S_4 \right.\\
&\quad \left. + S_4^{-1} + \sigma_h + \sigma_x + \sigma_y + \sigma_{d1} + \sigma_{d2}\right) v_2\\
&= \frac{1}{16}(v_2 + v_8 + v_9 + v_{15} + v_{30} + v_{19} + v_{21} + v_{28} + v_{31}\\
&\quad + v_{24} + v_{25} + v_{18} + v_{14} + v_3 + v_5 + v_{12})\\
&= P^{(1)}v_3 = P^{(1)}v_5 = P^{(1)}v_8 = P^{(1)}v_9 = P^{(1)}v_{12} = P^{(1)}v_{14}\\
&= P^{(1)}v_{15} = P^{(1)}v_{18} = P^{(1)}v_{19}\\
&= P^{(1)}v_{21} = P^{(1)}v_{24} = P^{(1)}v_{25} = P^{(1)}v_{28} = P^{(1)}v_{30} = P^{(1)}v_{31}
\end{aligned} \tag{4b}$$

$$\begin{aligned}
P^{(1)}v_6 &= \frac{1}{16}\left(e + C_4 + C_4^{-1} + C_2 + C_2^x + C_2^y + C_2^{d1} + C_2^{d2} + i + S_4 \right.\\
&\quad \left. + S_4^{-1} + \sigma_h + \sigma_x + \sigma_y + \sigma_{d1} + \sigma_{d2}\right) v_6\\
&= \frac{1}{16}(v_6 + v_7 + v_{10} + v_{11} + v_{26} + v_{23} + v_{22} + v_{27} + v_{27}\\
&\quad + v_{23} + v_{26} + v_{22} + v_{10} + v_7 + v_6 + v_{11})\\
&= \frac{2}{16}(v_6 + v_7 + v_{10} + v_{11} + v_{22} + v_{23} + v_{26} + v_{27})\\
&= P^{(1)}v_7 = P^{(1)}v_{10} = P^{(1)}v_{11} = P^{(1)}v_{22} = P^{(1)}v_{23}\\
&= P^{(1)}v_{26} = P^{(1)}v_{27}
\end{aligned} \tag{4c}$$

We may select any set of linearly independent symmetry-adapted freedoms as basis vectors for the subspace. Of the obtained 32 symmetry-adapted freedoms, there are only three linearly independent ones. Dropping the scalar multipliers (1/16 or 2/16) in the above expressions, the following three symmetry-adapted freedoms may be taken as the basis vectors of the first subspace:

Basis vectors for subspace $S^{(1)}$

$$\Phi_1^{(1)} = v_1 + v_4 + v_{13} + v_{16} + v_{17} + v_{20} + v_{29} + v_{32} \tag{5a}$$

$$\begin{aligned}
\Phi_2^{(1)} &= v_2 + v_3 + v_5 + v_8 + v_9 + v_{12} + v_{14} + v_{15} + v_{18} + v_{19} + v_{21}\\
&\quad + v_{24} + v_{25} + v_{28} + v_{30} + v_{31}
\end{aligned} \tag{5b}$$

$$\Phi_3^{(1)} = v_6 + v_7 + v_{10} + v_{11} + v_{22} + v_{23} + v_{26} + v_{27} \tag{5c}$$

Thus subspace $S^{(1)}$ of the 32-node cable-net system is 3-dimensional.

Similarly, the symmetry-adapted freedoms for subspace $S^{(2)}$ are obtained on the basis of idempotent $P^{(2)}$. Using the expression for $P^{(2)}$ as given by Eq. (3b), and applying its symmetry operations on each freedom v_i ($i = 1,\ 2,\ ...,\ 32$) in turn, we obtain 32 symmetry-adapted freedoms as follows:

$$\begin{aligned} P^{(2)}v_1 &= \frac{1}{16}\big(e + C_4 + C_4^{-1} + C_2 - C_2^x - C_2^y - C_2^{d1} - C_2^{d2} + i + S_4 \\ &\quad + S_4^{-1} + \sigma_h - \sigma_x - \sigma_y - \sigma_{d1} - \sigma_{d2}\big)\, v_1 \\ &= \frac{1}{16}(v_1 + v_4 + v_{13} + v_{16} - v_{29} - v_{20} - v_{17} - v_{32} + v_{32} \\ &\quad + v_{20} + v_{29} + v_{17} - v_{13} - v_4 - v_1 - v_{16}) \\ &= 0 = P^{(2)}v_4 = P^{(2)}v_{13} = P^{(2)}v_{16} = P^{(2)}v_{17} = P^{(2)}v_{20} \\ &= P^{(2)}v_{29} = P^{(2)}v_{32} \end{aligned} \tag{6a}$$

$$\begin{aligned} P^{(2)}v_2 &= \frac{1}{16}\big(e + C_4 + C_4^{-1} + C_2 - C_2^x - C_2^y - C_2^{d1} - C_2^{d2} + i + S_4 \\ &\quad + S_4^{-1} + \sigma_h - \sigma_x - \sigma_y - \sigma_{d1} - \sigma_{d2}\big)\, v_2 \\ &= \frac{1}{16}(v_2 + v_8 + v_9 + v_{15} - v_{30} - v_{19} - v_{21} - v_{28} + v_{31} \\ &\quad + v_{24} + v_{25} + v_{18} - v_{14} - v_3 - v_5 - v_{12}) \\ &= -P^{(2)}v_3 = -P^{(2)}v_5 = P^{(2)}v_8 = P^{(2)}v_9 = -P^{(2)}v_{12} \\ &= -P^{(2)}v_{14} = P^{(2)}v_{15} = P^{(2)}v_{18} = -P^{(2)}v_{19} \\ &= -P^{(2)}v_{21} = P^{(2)}v_{24} = P^{(2)}v_{25} = -P^{(2)}v_{28} \\ &= -P^{(2)}v_{30} = P^{(2)}v_{31} \end{aligned} \tag{6b}$$

$$\begin{aligned} P^{(2)}v_6 &= \frac{1}{16}\big(e + C_4 + C_4^{-1} + C_2 - C_2^x - C_2^y - C_2^{d1} - C_2^{d2} + i + S_4 \\ &\quad + S_4^{-1} + \sigma_h - \sigma_x - \sigma_y - \sigma_{d1} - \sigma_{d2}\big)\, v_6 \\ &= \frac{1}{16}(v_6 + v_7 + v_{10} + v_{11} - v_{26} - v_{23} - v_{22} - v_{27} + v_{27} \\ &\quad + v_{23} + v_{26} + v_{22} - v_{10} - v_7 - v_6 - v_{11}) \\ &= 0 = P^{(2)}v_7 = P^{(2)}v_{10} = P^{(2)}v_{11} = P^{(2)}v_{22} = P^{(2)}v_{23} \\ &= P^{(2)}v_{26} = P^{(2)}v_{27} \end{aligned} \tag{6c}$$

There are 16 non-zero symmetry-adapted freedoms, which are all linearly dependent (either identical to each other or only different with regard to sign). We therefore have only one independent symmetry-adapted freedom. Disregarding the scalar multiplier 1/16, the following symmetry-adapted freedom may be taken as the basis vector of the second subspace:

Basis vector for subspace $S^{(2)}$

$$\begin{aligned} \Phi_1^{(2)} &= v_2 - v_3 - v_5 + v_8 + v_9 - v_{12} - v_{14} + v_{15} + v_{18} - v_{19} - v_{21} \\ &\quad + v_{24} + v_{25} - v_{28} - v_{30} + v_{31} \end{aligned} \tag{7}$$

Thus subspace $S^{(2)}$ of the 32-node cable-net system is 1-dimensional. We proceed in the same way for the rest of the subspaces of the problem, using the idempotent for each subspace (i.e. idempotent $P^{(j)}$ for subspace $S^{(j)}$) to generate the symmetry-adapted freedoms for that subspace, and then selecting a set of linearly independent symmetry-adapted freedoms as the basis vectors for the subspace. The results are as follows:

Basis vector for subspace $S^{(3)}$

$$\begin{aligned} \Phi_1^{(3)} &= v_2 + v_3 - v_5 - v_8 - v_9 - v_{12} + v_{14} + v_{15} + v_{18} + v_{19} \\ &\quad - v_{21} - v_{24} - v_{25} - v_{28} + v_{30} + v_{31} \end{aligned} \tag{8}$$

Basis vectors for subspace $S^{(4)}$

$$\Phi_1^{(4)} = v_1 - v_4 - v_{13} + v_{16} + v_{17} - v_{20} - v_{29} + v_{32} \tag{9a}$$

$$\begin{aligned} \Phi_2^{(4)} &= v_2 - v_3 + v_5 - v_8 - v_9 + v_{12} - v_{14} + v_{15} + v_{18} - v_{19} \\ &\quad + v_{21} - v_{24} - v_{25} + v_{28} - v_{30} + v_{31} \end{aligned} \tag{9b}$$

$$\Phi_3^{(4)} = v_6 - v_7 - v_{10} + v_{11} + v_{22} - v_{23} - v_{26} + v_{27} \tag{9c}$$

Basis vectors for subspace $S^{(5)}$

$$\Phi_1^{(5)} = v_1 - v_{16} - v_{17} + v_{32} \tag{10a}$$

$$\Phi_2^{(5)} = v_2 - v_{15} - v_{18} + v_{31} \tag{10b}$$

$$\Phi_3^{(5)} = v_3 - v_{14} - v_{19} + v_{30} \tag{10c}$$

$$\Phi_4^{(5)} = v_4 - v_{13} - v_{20} + v_{29} \tag{10d}$$

$$\Phi_5^{(5)} = v_5 - v_{12} - v_{21} + v_{28} \tag{10e}$$

$$\Phi_6^{(5)} = v_6 - v_{11} - v_{22} + v_{27} \tag{10f}$$

$$\Phi_7^{(5)} = v_7 - v_{10} - v_{23} + v_{26} \tag{10g}$$

$$\Phi_8^{(5)} = v_8 - v_9 - v_{24} + v_{25} \tag{10h}$$

Basis vectors for subspace $S^{(6)}$

$$\begin{aligned} \Phi_1^{(6)} &= v_2 - v_3 - v_5 + v_8 + v_9 - v_{12} - v_{14} + v_{15} - v_{18} + v_{19} \\ &\quad + v_{21} - v_{24} - v_{25} + v_{28} + v_{30} - v_{31} \end{aligned} \tag{11}$$

Basis vectors for subspace $S^{(7)}$

$$\Phi_1^{(7)} = v_1 + v_4 + v_{13} + v_{16} - v_{17} - v_{20} - v_{29} - v_{32} \tag{12a}$$

$$\begin{aligned} \Phi_2^{(7)} &= v_2 + v_3 + v_5 + v_8 + v_9 + v_{12} + v_{14} + v_{15} - v_{18} - v_{19} \\ &\quad - v_{21} - v_{24} - v_{25} - v_{28} - v_{30} - v_{31} \end{aligned} \tag{12b}$$

$$\Phi_3^{(7)} = v_6 + v_7 + v_{10} + v_{11} - v_{22} - v_{23} - v_{26} - v_{27} \tag{12c}$$

Basis vectors for subspace $S^{(8)}$

$$\Phi_1^{(8)} = v_1 - v_4 - v_{13} + v_{16} - v_{17} + v_{20} + v_{29} - v_{32} \tag{13a}$$

$$\begin{aligned} \Phi_2^{(8)} &= v_2 - v_3 + v_5 - v_8 - v_9 + v_{12} - v_{14} + v_{15} - v_{18} + v_{19} \\ &\quad - v_{21} + v_{24} + v_{25} - v_{28} + v_{30} - v_{31} \end{aligned} \tag{13b}$$

$$\Phi_3^{(8)} = v_6 - v_7 - v_{10} + v_{11} - v_{22} + v_{23} + v_{26} - v_{27} \tag{13c}$$

Basis vector for subspace $S^{(9)}$

$$\begin{aligned} \Phi_1^{(9)} &= v_2 + v_3 - v_5 - v_8 - v_9 - v_{12} + v_{14} + v_{15} - v_{18} - v_{19} \\ &\quad + v_{21} + v_{24} + v_{25} + v_{28} - v_{30} - v_{31} \end{aligned} \tag{14}$$

Basis vectors for subspace $S^{(10)}$

$$\Phi_1^{(10)} = v_1 - v_{16} + v_{17} - v_{32} \tag{15a}$$

$$\Phi_2^{(10)} = v_2 - v_{15} + v_{18} - v_{31} \tag{15b}$$

$$\Phi_3^{(10)} = v_3 - v_{14} + v_{19} - v_{30} \tag{15c}$$

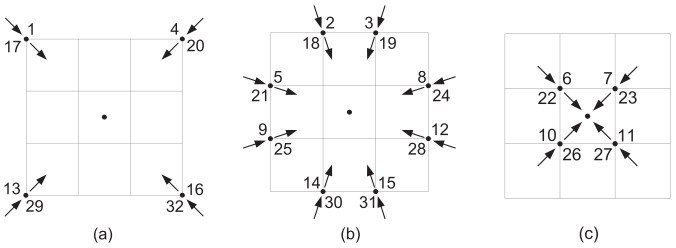

Fig. 8. Basis vectors of subspace $S^{(1)}$ of the 32-node double-layer cable net: (a) $\Phi_1^{(1)}$; (b) $\Phi_2^{(1)}$and (c) $\Phi_3^{(1)}$.

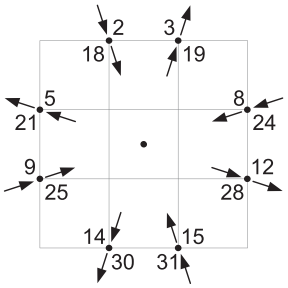

Fig. 9. Basis vector of subspace $S^{(2)}$ of the 32-node double-layer cable net: $\Phi_1^{(2)}$.

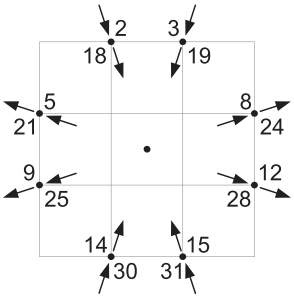

Fig. 10. Basis vector of subspace $S^{(3)}$ of the 32-node double-layer cable net: $\Phi_1^{(3)}$.

$$\Phi_4^{(10)} = v_4 - v_{13} + v_{20} - v_{29} \tag{15d}$$

$$\Phi_5^{(10)} = v_5 - v_{12} + v_{21} - v_{28} \tag{15e}$$

$$\Phi_6^{(10)} = v_6 - v_{11} + v_{22} - v_{27} \tag{15f}$$

$$\Phi_7^{(10)} = v_7 - v_{10} + v_{23} - v_{26} \tag{15g}$$

$$\Phi_8^{(10)} = v_8 - v_9 + v_{24} - v_{25} \tag{15h}$$

The symmetry types of the 10 subspaces of the problem may be visualised by plotting the coordinates of the basis vectors at the nodes of the double-layer grid. Figs. 8–17 show such basis-vector plots for all the subspaces. The grid lines in the diagrams correspond to those of Fig. 6, but in plotting a given basis vector, only the nodes associated with the components of the basis vector are shown as black dots at the corresponding nodal locations on the grid. As an example, basis vector $\Phi_1^{(1)}$of subspace $S^{(1)}$ has eight components $\{v_1,v_4,v_{13},v_{16},v_{17},v_{20},v_{29},v_{32}\}$ as given by Eq. (5a), so in Fig. 8(a), only the nodes {1, 4, 13, 16, 17, 20, 29, 32} are shown in the diagram. In all the diagrams, the centre of symmetry of the configuration is marked by the dot in the middle. The numbering of the nodes and the plotting of basis-vector components is in accordance with the following convention:

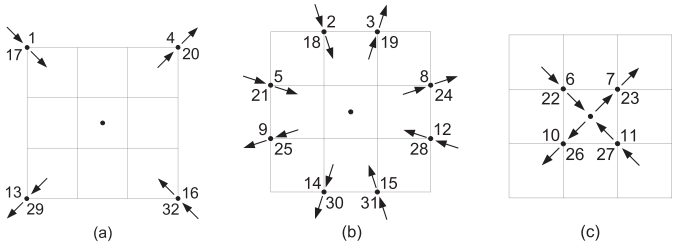

Fig. 11. Basis vectors of subspace $S^{(4)}$ of the 32-node double-layer cable net: (a) $\Phi_1^{(4)}$; (b) $\Phi_2^{(4)}$and (c) $\Phi_3^{(4)}$.

1. At a given nodal location (marked by a black dot), the smaller number (in the range 1–16) always refers to the top-layer node, while the larger number (in the range 17–32) refers to the bottom-layer node. The numbers refer to the nodal location (i.e. the dot), not the arrows.
2. At a given nodal location, the outer arrow refers to the node in the top layer of the cable net; the inner arrow refers to the node in the bottom layer of the cable net.
3. Arrows pointing *towards* the centre of the diagram denote *positive* basis-vector components; arrows pointing *away* from the centre denote *negative* basis-vector components.
4. The components of symmetry-adapted freedoms are actually vertical displacements at the relevant nodes of the cable net. Positive values of components of symmetry-adapted freedoms (i.e. positive values of basis-vector components) correspond to vertical displacements towards the central horizontal plane of symmetry of the double-layer configuration (i.e. downward movement for top-layer nodes and upward movement for bottom-layer nodes).

We observe that basis vectors belonging to the same subspace have the same symmetry type, and this symmetry type (combinations of symmetry and anti-symmetry properties with respect to the one horizontal and four vertical planes of symmetry) is different for each subspace. In mathematical terms, a basis vector belonging to a given subspace will be orthogonal to every other vector that does not belong to the same subspace. When the double-layer grid experiences small vertical vibrations, the observed modes of vibration will conform to these same symmetry types. We will come back to this point later.

Subspaces $S^{(5)}$ and $S^{(10)}$ are associated with 2-dimensional irreducible representations E_g and E_u of the symmetry group D_{4h} (refer to Table 2). We therefore expect these subspaces to be associated with repeated eigenvalues. Taking subspace $S^{(5)}$, it should be possible to linearly combine the basis vectors spanning the subspace in such a way that we create two new sets of vectors that are orthogonal to each other. This is equivalent to a conceptual splitting of subspace $S^{(5)}$ (with 8 basis vectors) into smaller subspaces $S^{(5A)}$ and $S^{(5B)}$ that each have 4 basis vectors. The required linear combinations are obtained by inspection as follows:

Basis vectors for subspace $S^{(5A)}$

$$\Phi_1^{(5A)} = \Phi_1^{(5)} = v_1 - v_{16} - v_{17} + v_{32} \tag{16a}$$

$$\Phi_2^{(5A)} = \Phi_6^{(5)} = v_6 - v_{11} - v_{22} + v_{27} \tag{16b}$$

$$\Phi_3^{(5A)} = \Phi_2^{(5)} + \Phi_5^{(5)} = v_2 + v_5 - v_{12} - v_{15} - v_{18} - v_{21} + v_{28} + v_{31} \tag{16c}$$

$$\Phi_4^{(5A)} = \Phi_3^{(5)} - \Phi_8^{(5)} = v_3 - v_8 + v_9 - v_{14} - v_{19} + v_{24} - v_{25} + v_{30} \tag{16d}$$

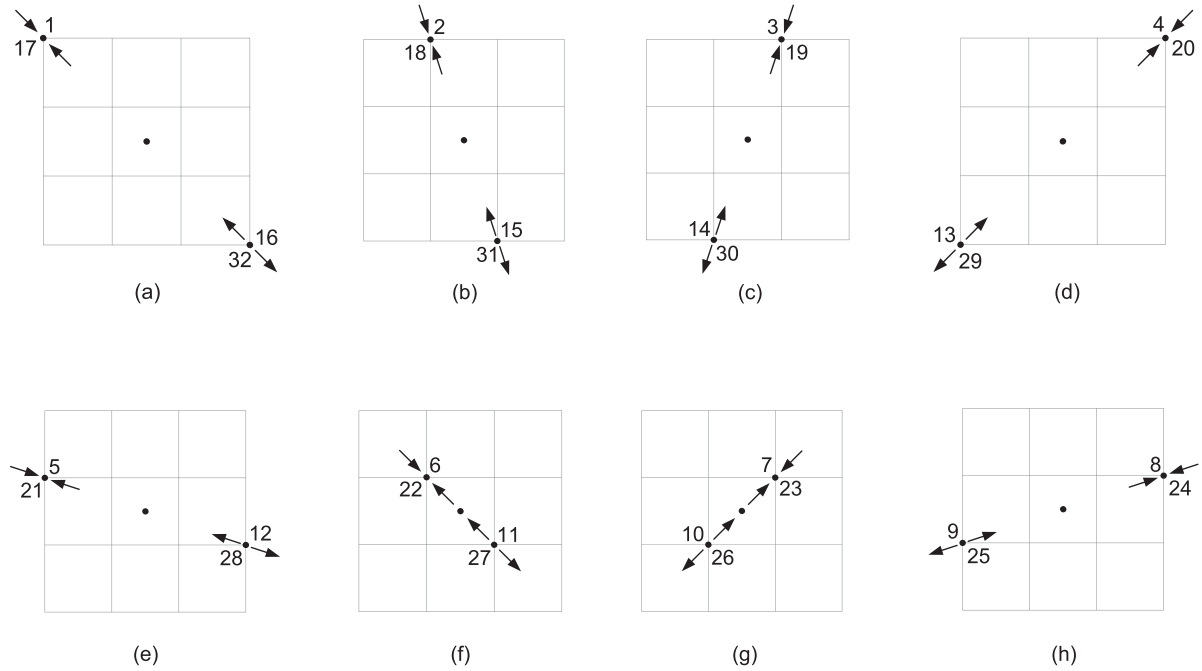

Fig. 12. Basis vectors of subspace $S^{(5)}$ of the 32-node double-layer cable net: (a) $\Phi_1^{(5)}$; (b) $\Phi_2^{(5)}$; (c) $\Phi_3^{(5)}$; (d) $\Phi_4^{(5)}$; (e) $\Phi_5^{(5)}$; (f) $\Phi_6^{(5)}$; (g) $\Phi_7^{(5)}$ and (h) $\Phi_8^{(5)}$.

Basis vectors for subspace $S^{(5B)}$

$$\Phi_1^{(5B)} = \Phi_4^{(5)} = v_4 - v_{13} - v_{20} + v_{29} \tag{17a}$$

$$\Phi_2^{(5B)} = \Phi_7^{(5)} = v_7 - v_{10} - v_{23} + v_{26} \tag{17b}$$

$$\Phi_3^{(5B)} = \Phi_2^{(5)} - \Phi_5^{(5)} = v_2 - v_5 + v_{12} - v_{15} - v_{18} + v_{21} - v_{28} + v_{31} \tag{17c}$$

$$\Phi_4^{(5B)} = \Phi_3^{(5)} + \Phi_8^{(5)} = v_3 + v_8 - v_9 - v_{14} - v_{19} - v_{24} + v_{25} + v_{30} \tag{17d}$$

The orthogonality of the above new sets of vectors are evident when we compare the plots in Fig. 18 (basis vectors for subspace $S^{(5A)}$) versus those in Fig. 19 (basis vectors for subspace $S^{(5B)}$). In these plots, a solid diagonal line in the central panel of the cable net denotes a symmetry plane of the vector pattern, while a dashed line denotes an antisymmetry plane. We note that all four vectors belonging to the same subspace have the same symmetry and antisymmetry planes. Furthermore, the symmetry and antisymmetry planes of the vectors of subspace $S^{(5A)}$ are perpendicular to their counterparts in subspace $S^{(5B)}$, confirming the orthogonality of the two sets of vectors.

Similarly, we may split subspace $S^{(10)}$ (with 8 basis vectors) into independent smaller subspaces $S^{(10A)}$ and $S^{(10B)}$ that each have 4 basis vectors, as follows:

Basis vectors for subspace $S^{(10A)}$

$$\Phi_1^{(10A)} = \Phi_1^{(10)} = v_1 - v_{16} + v_{17} - v_{32} \tag{18a}$$

$$\Phi_2^{(10A)} = \Phi_6^{(10)} = v_6 - v_{11} + v_{22} - v_{27} \tag{18b}$$

$$\Phi_3^{(10A)} = \Phi_2^{(10)} + \Phi_5^{(10)} = v_2 + v_5 - v_{12} - v_{15} + v_{18} + v_{21} - v_{28} - v_{31} \tag{18c}$$

$$\Phi_4^{(10A)} = \Phi_3^{(10)} - \Phi_8^{(10)} = v_3 - v_8 + v_9 - v_{14} + v_{19} - v_{24} + v_{25} - v_{30} \tag{18d}$$

Basis vectors for subspace $S^{(10B)}$

$$\Phi_1^{(10B)} = \Phi_4^{(10)} = v_4 - v_{13} + v_{20} - v_{29} \tag{19a}$$

$$\Phi_2^{(10B)} = \Phi_7^{(10)} = v_7 - v_{10} + v_{23} - v_{26} \tag{19b}$$

$$\Phi_3^{(10B)} = \Phi_2^{(10)} - \Phi_5^{(10)} = v_2 - v_5 + v_{12} - v_{15} + v_{18} - v_{21} + v_{28} - v_{31} \tag{19c}$$

$$\Phi_4^{(10B)} = \Phi_3^{(10)} + \Phi_8^{(10)} = v_3 + v_8 - v_9 - v_{14} + v_{19} + v_{24} - v_{25} - v_{30} \tag{19d}$$

The orthogonality of the two sets of basis vectors may be seen by comparing the plots of Fig. 20 versus those of Fig. 21. The symmetry and antisymmetry planes of the basis vectors of subspace $S^{(10A)}$ (shown in Fig. 20) are perpendicular to those of the basis vectors of subspace $S^{(10B)}$ (shown in Fig. 21), confirming the orthogonality of the two sets. Vectors belonging to the same subspace clearly have the same symmetry and antisymmetry planes.

5. Insights and computational benefits

Through the group-theoretic procedure described in the previous section, the original vector space of the problem, spanned by 32 basis vectors representing the vertical degrees of freedom at the 32 nodes of the double-layer cable net (16 nodes per layer), has been decomposed into 12 independent subspaces each of much smaller dimension (i.e. number of basis vectors) as summarised in Table 3.

Table 3 shows that, instead of solving a 32-dimensional eigenvalue problem (i.e. one with 32 degrees of freedom), the achieved decomposition requires the solution of 12 independent eigenvalue

Table 3
Dimensions of subspaces of the 32-node double-layer cable net.

Subspace	Dimension
$S^{(1)}$	3
$S^{(2)}$	1
$S^{(3)}$	1
$S^{(4)}$	3
$S^{(5A)}$	4
$S^{(5B)}$	4
$S^{(6)}$	1
$S^{(7)}$	3
$S^{(8)}$	3
$S^{(9)}$	1
$S^{(10A)}$	4
$S^{(10B)}$	4
Full space	32

problems of much smaller dimensions, which represents a very substantial reduction in computational effort. We will consider the issue of computational effort in more detail very shortly.

Let us revisit the subspace pairs $\{S^{(5A)};\ S^{(5B)}\}$ and $\{S^{(10A)};\ S^{(10B)}\}$. An examination of the vector plots in Figs 18–21 reveals that the sets of basis vectors for subspaces $S^{(5A)}$ and $S^{(5B)}$ are identical to each other, except for their different orientations of symmetry and antisymmetry planes. Similarly, the sets of basis vectors for subspaces $S^{(10A)}$ and $S^{(10B)}$ are identical to each other, except for orientation. The orientation of a set of basis vectors does not affect the physical properties of the subspace, so we conclude that subspaces $S^{(5A)}$ and $S^{(5B)}$ will yield identical sets of eigenvalues. Similarly, subspaces $S^{(10A)}$ and $S^{(10B)}$ will yield identical sets of eigenvalues.

Thus in conducting a vibration analysis, we do not need to consider both subspaces $S^{(5A)}$ and $S^{(5B)}$. Consideration of either of these 4-dimensional subspaces will yield all the 8 natural frequencies of subspace $S^{(5)}$, which occur as four sets of repeated roots. Similarly, consideration of either subspace $S^{(10A)}$ or subspace $S^{(10B)}$ will yield all the 8 natural frequencies of subspace $S^{(10)}$, which also occur as four sets of repeated roots. The linear combinations of equation sets (16, 17) and (18, 19) provide a direct way of obtaining repeated eigenvalues of the 8-dimensional subspaces $S^{(5)}$ and $S^{(10)}$ without tackling the full eigenvalue problem of these subspaces.

In eigenvalue problems of the vibration of structural systems with discrete parameters and a finite number of degrees of freedom, the computational effort associated with extracting all the natural frequencies of the system is very much a function of the total number of degrees of freedom n of the system, and may generally be considered as roughly proportional to n^3, the exact relationship depending, of course, on the computational method used. By decomposing the original vector space of the problem (spanned by n basis vectors corresponding to the n degrees of freedom of the system) into r independent subspaces of dimensions $\{n_1, n_2, ..., n_r\}$, where

$$n_1 + n_2 + \ \ldots\ + n_r = n \tag{20}$$

we achieve a reduction in computational effort which we may represent as a ratio R_{ce} as follows:

$$R_{ce} = \frac{n_1^3 + n_2^3 + \ \cdots\ + n_r^3}{n^3} \ \leq\ 1.0 \tag{21}$$

For the decomposition in Table 3, we get

$$R_{ce} = \frac{1}{32^3}\left(3^3 + 1^3 + 1^3 + 3^3 + 4^3 + 0 + 1^3 + 3^3 + 3^3 + 1^3 + 4^3 + 0\right)$$
$$= \frac{240}{32768} = 0.0073 \tag{22}$$

the zero terms signifying that computations for subspaces $S^{(5B)}$ and $S^{(10B)}$ are not required once the results for subspaces $S^{(5A)}$ and $S^{(10A)}$ have been computed. Thus our group-theoretic decomposition reduces the computational effort to a mere 0.73% of the computational effort associated with the full problem of the 32 degree-of-freedom double-layer cable net.

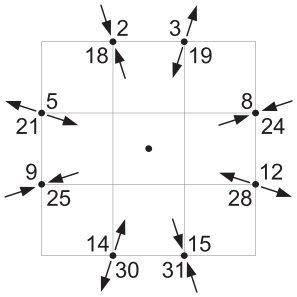

Fig. 13. Basis vector of subspace $S^{(6)}$ of the 32-node double-layer cable net: $\Phi_1^{(6)}$.

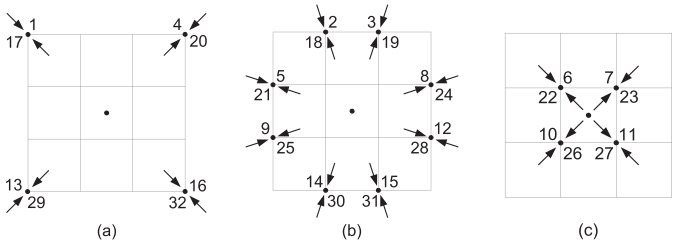

Fig. 14. Basis vectors of subspace $S^{(7)}$ of the 32-node double-layer cable net: (a) $\Phi_1^{(7)}$; (b) $\Phi_2^{(7)}$ and (c) $\Phi_3^{(7)}$.

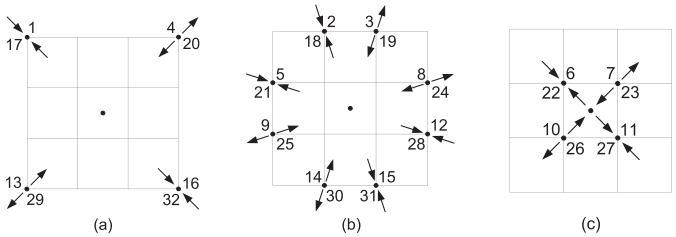

Fig. 15. Basis vectors of subspace $S^{(8)}$ of the 32-node double-layer cable net: (a) $\Phi_1^{(8)}$; (b) $\Phi_2^{(8)}$ and (c) $\Phi_3^{(8)}$.

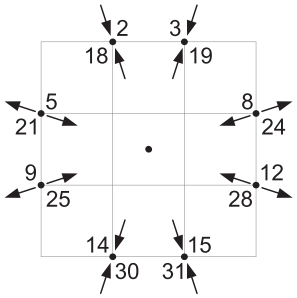

Fig. 16. Basis vector of subspace $S^{(9)}$ of the 32-node double-layer cable net: $\Phi_1^{(9)}$.

Apart from these very substantial computational gains, some important insights on the vibration behaviour of the double-layer cable net can also be gained prior to any eigenvalue calculations. First and foremost, the patterns of vibration are not haphazard, but conform to specific symmetry types associated with the symmetry group D_{4h}. For the example that has been considered, the modes of vibration will have patterns that are similar to the plots of basis vectors shown in Figs 8–11, 13–16 and 18–21. For the top-layer nodes, and at any given time, the vectors pointing *towards* the centre of symmetry of the plots denote *downward* motion, while the

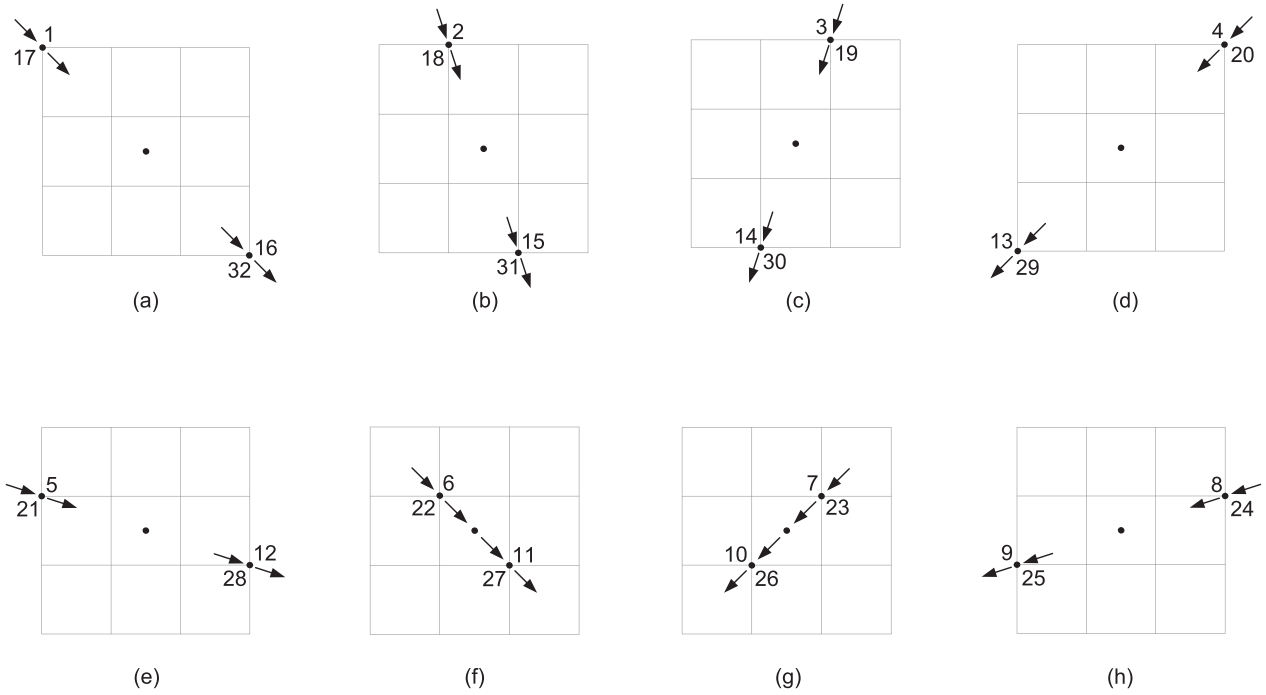

Fig. 17. Basis vectors of subspace $S^{(10)}$ of the 32-node double-layer cable net: (a) $\Phi_1^{(10)}$; (b) $\Phi_2^{(10)}$; (c) $\Phi_3^{(10)}$; (d) $\Phi_4^{(10)}$; (e) $\Phi_5^{(10)}$; (f) $\Phi_6^{(10)}$; (g) $\Phi_7^{(10)}$ and (h) $\Phi_8^{(10)}$.

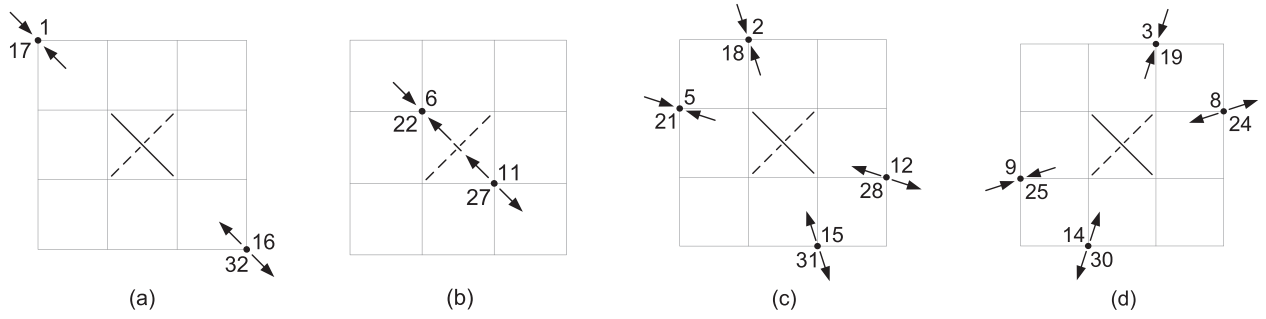

Fig. 18. Basis vectors of subspace $S^{(5A)}$ of the 32-node double-layer cable net: (a) $\Phi_1^{(5A)}$; (b) $\Phi_2^{(5A)}$; (c) $\Phi_3^{(5A)}$ and (d) $\Phi_4^{(5A)}$.

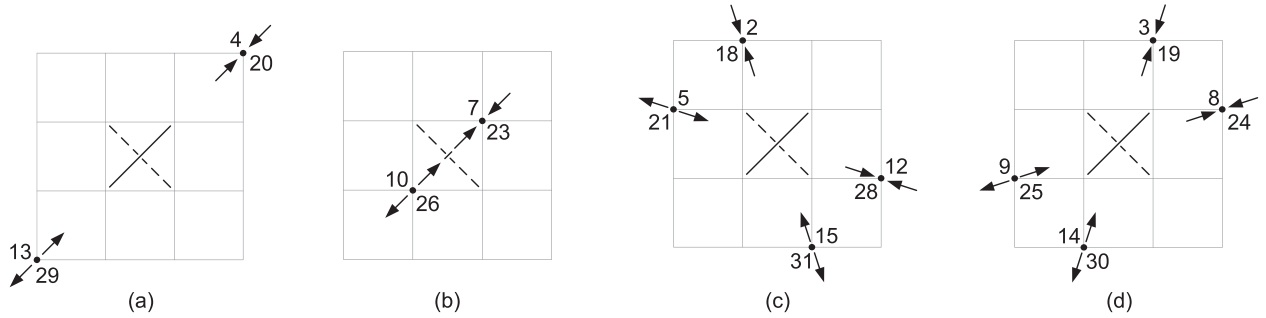

Fig. 19. Basis vectors of subspace $S^{(5B)}$ of the 32-node double-layer cable net: (a) $\Phi_1^{(5B)}$; (b) $\Phi_2^{(5B)}$; (c) $\Phi_3^{(5B)}$ and (d) $\Phi_4^{(5B)}$.

vectors pointing *away* from the centre of symmetry of the plots denote *upward* motion, and vice-versa for the bottom-layer nodes.

Secondly, and equally important, the foregoing group-theoretic analysis informs us, before any calculations for natural frequencies and mode shapes are actually performed, on how many mode shapes there will be of a given symmetry type. For example, of the 32 vibration modes of our example, 3 modes will belong to subspace $S^{(1)}$ having the full symmetry of a square prism. In these modes, the corner nodes {1, 4, 13, 16, 17, 20, 29, 32} will all move simultaneously outwards or inwards (with respect to the central *xy* plane of symmetry) with the same amplitude A_1, the mid-side nodes {2, 3, 5, 8, 9, 12, 14, 15, 18, 19, 21, 24, 25, 28, 30, 31} will all move simultaneously outwards or inwards with the same amplitude A_2, and the centre nodes {6, 7, 10, 11, 22, 23, 26, 27} will all move simultaneously outwards or inwards with the same amplitude A_3, bearing in mind that all nodes of a given set carry equal masses (m_1, m_2 or m_3) and are connected by equal stiffnesses (k_1, k_2 or k_3). Thus in this subspace, there will be three distinct patterns of motion, all with full D_{4h} symmetry. These three modes are an example of the transverse extensional

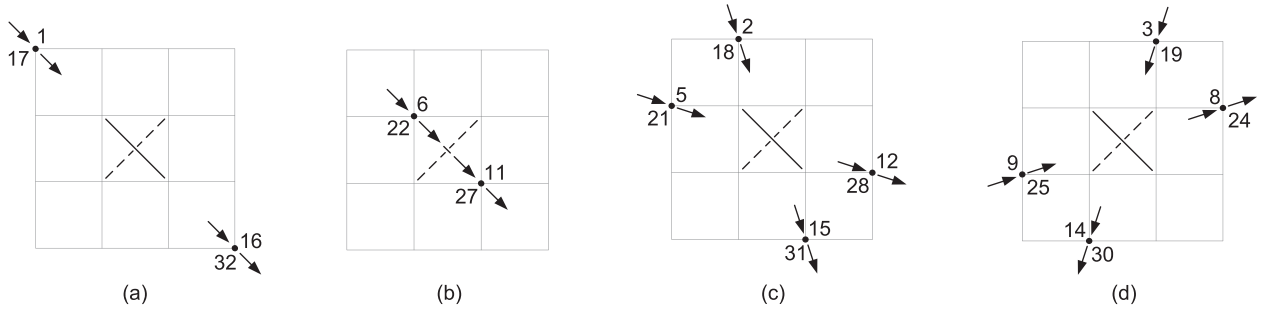

Fig. 20. Basis vectors of subspace $S^{(10A)}$ of the 32-node double-layer cable net: (a) $\Phi_1^{(10A)}$; (b) $\Phi_2^{(10A)}$; (c) $\Phi_3^{(10A)}$ and (d) $\Phi_4^{(10A)}$.

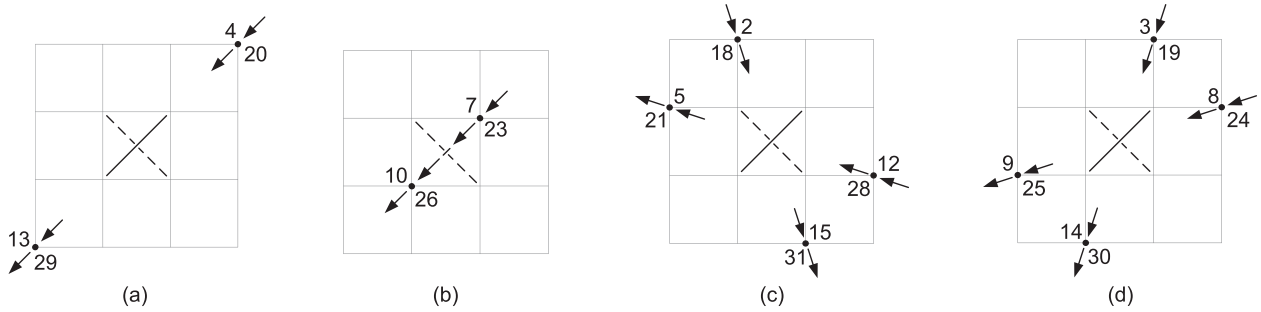

Fig. 21. Basis vectors of subspace $S^{(10B)}$ of the 32-node double-layer cable net: (a) $\Phi_1^{(10B)}$; (b) $\Phi_2^{(10B)}$; (c) $\Phi_3^{(10B)}$ and (d) $\Phi_4^{(10B)}$.

(or "breathing") modes that were mentioned in Section 1, which are characterised by expansion and contraction of the vertical distance between the two layers.

Thirdly, the group-theoretic analysis reveals the existence of pairs of modes that have identical shapes (except for orientation of symmetry and anti-symmetry planes) and identical values of natural frequencies. As already pointed out in the previous section, there are four such pairs in each of subspaces $S^{(5)}$ and $S^{(10)}$. A numerical analysis would not be able to distinguish these.

Finally, with this insight on the symmetry types of the modes associated with each of the subspaces of the double-layer cable net, if we were only interested in the natural frequencies of modes having a particular shape, we would only need to focus attention on the associated subspace, and solve for the eigenvalues of that subspace only, instead of having to tackle the full problem first, and then pick out the required modes at the end. In this regard, it must be noted that the eigenvalues yielded by the independent subspaces are, in fact, the required eigenvalues of the full problem.

Evidently, the 32-node double-layer cable net could have been studied on the basis of symmetry group D_{2h}, which is a sub-group of D_{4h}, and describes the symmetry of a rectangular prism. The idempotents of group D_{2h} were given as Eqs. (2). Applying idempotent $P^{(1)}$ of symmetry group D_{2h} (as given by Eq. (2a)) to each of the 32 nodal freedoms of the cable net yields only four independent basis vectors for subspace $S^{(1)}$, which may be taken as

$$\Phi_1^{(1)} = \nu_1 + \nu_{16} + \nu_{29} + \nu_{20} + \nu_{32} + \nu_{17} + \nu_{13} + \nu_4 \tag{23a}$$

$$\Phi_2^{(1)} = \nu_2 + \nu_{15} + \nu_{30} + \nu_{19} + \nu_{31} + \nu_{18} + \nu_{14} + \nu_3 \tag{23b}$$

$$\Phi_3^{(1)} = \nu_5 + \nu_{12} + \nu_{25} + \nu_{24} + \nu_{28} + \nu_{21} + \nu_9 + \nu_8 \tag{23c}$$

$$\Phi_4^{(1)} = \nu_6 + \nu_{11} + \nu_{26} + \nu_{23} + \nu_{27} + \nu_{22} + \nu_{10} + \nu_7 \tag{23d}$$

Similarly, applying idempotents $P^{(2)} - P^{(8)}$ of symmetry group D_{2h} (as given by Eqs. (2b)–(2h)) to the nodal freedoms of the cable net yields four independent basis vectors for each of subspaces $S^{(2)} - S^{(8)}$. Thus symmetry group D_{2h} decomposes the same problem into 8 subspaces each of dimension 4. For this group, the reduction factor for computational effort is

$$R_{ce} = \frac{1}{32^3}\left(4^3 + 4^3 + 4^3 + 4^3 + 4^3 + 4^3 + 4^3 + 4^3\right) = \frac{512}{32768} = 0.0156 \tag{24}$$

(i.e. 1.56%). This is not as efficient as the D_{4h} decomposition, since not all symmetries of the cable net are utilised, and modes of the same natural frequency (i.e. doubly repeating roots) are not automatically identified. Nevertheless, the advantage of group D_{2h} over D_{4h} is that computational effort is evenly spread over the 8 subspaces (all are of dimension 4), unlike the D_{4h} decomposition where the dimensions of the subspaces vary from 1 to 4. For large-scale problems where it might be desired to make use of parallel processors to speed up computations, considerations of distribution of computational effort over the various subspaces become more important.

6. Concluding remarks

Coupling high-tension cable nets into double-layer configurations offers the opportunity for modifying the vibration characteristics of single-layer cable nets in a beneficial way, when members of appropriate damping and stiffness properties are employed as coupling devices. This investigation has focussed on double-layer cable nets of D_{4h} symmetry, and has employed group theory to gain some important insights on the vibration characteristics of such configurations. These insights have included the type of symmetries which the vibration modes are going to have, the number of modes that will exhibit a given type of symmetry, the existence of pairs of modes of the same natural frequency, and the nature of the symmetry associated with such paired modes.

By examining the dimensions of the various subspaces into which the original vector space of the problem decomposes, it has been possible to obtain an estimate of the reduction in computational effort afforded through use of group theory. Although the

study was conducted on the basis of a double-layer cable net with a particular number of nodes (i.e. 32), we may extrapolate the conclusions to much larger cable nets, as the pattern of vector-space decomposition remains the same. A large D_{4h} double-layer cable net might have, for example, 200 cables running in each of the x and y directions, giving 40, 000 nodes per layer, or 80, 000 degrees of freedom in total.

For double-layer cable nets of the type considered in this study, use of the symmetry group D_{4h} reduces the computational effort involved in calculating natural frequencies and mode shapes to only 0.7% of that associated with the conventional approach. On the other hand, use of the sub-group D_{2h}, which is of half the order, also results in a substantial but smaller reduction of computational effort (of the order of 1.6% of that associated with the conventional approach), and does not offer as many insights into vibration behaviour as symmetry group D_{4h}. However, the simpler D_{2h} group results in a more uniform decomposition of the original space of the problem, an important consideration in large-scale problems where parallel processors may need to be used.

The considerations of this paper are relevant to the study of the vibration behaviour of cable-net systems of the type used for roofing applications. It is very important for engineers to understand the vibration characteristics of slender structures such as long-span cable-net roofs, in order to avoid wind-induced resonance and other adverse effects. If excessive vibrations are envisaged, then it may be necessary to install suitable damping devices; a full understanding of the behaviour of the undamped system is the first step in the design of an effective damping system. While the vibration properties of a cable net can be quantified from a conventional analysis, use of group-theory allows important features of the behaviour to be predicted before detailed calculations are performed. Unlike single-layer cable nets and layered space grids, double-layer cable nets with soft (i.e. spring-like) transverse coupling feature transverse-stretching modes of vibration, and group theory is particularly effective in studying these. This paper has revealed the symmetry types of such modes.

In a follow-up study, with the calculation of natural frequencies and mode shapes in mind, we will formulate the eigenvalue problem of the double-layer cable net on the basis of group-theory, solve this in terms of the cable forces and coupling stiffnesses, and evaluate the influence of coupling stiffnesses on the vibration characteristics of layered cable nets. Use of group theory in the calculation stages results in decomposition of the eigenvalue problem into a series of independent smaller problems, with consequent reductions in the computational effort involved in the determination of natural frequencies and mode shapes. The symmetry of double-layer cable nets of the present type is of higher order than that of the constituent single-layer cable nets, so the computational gains will be considerably higher.

References

Buchholdt, H.A., Davies, M., Hussey, M.J.L., 1968. The analysis of cable nets. J. Inst. Math. Appl. 4, 339–358.

Calladine, C.R., 1982. Modal stiffnesses of a pretensioned cable net. Int. J. Solids Struct. 18, 829–846.

Chen, Y., Feng, J., 2012. Generalized eigenvalue analysis of symmetric prestressed structures using group theory. J. Comput. Civil Eng. 26 (4), 488–497.

Chen, Y., Feng, J., 2016. Improved symmetry method for the mobility of regular structures using graph products. J. Struct. Eng. 142, 04016051.

Chen, Y., Feng, J., Ma, R., Zhang, Y., 2015a. Efficient symmetry method for calculating integral prestress modes of statically indeterminate cable-strut structures. J. Struct. Eng. 141 (10), 04014240.

Chen, Y., Sareh, P., Feng, J., 2015b. Effective insights into the geometric stability of symmetric skeletal structures under symmetric variations. Int. J. Solids Struct. 69/70, 277–290.

Fowler, P.W., Guest, S.D., 2000. A symmetry extension of Maxwell's rule for rigidity of frames. Int. J. Solids Struct. 37 (12), 1793–1804.

Guest, S.D., Fowler, P.W., 2007. Symmetry conditions and finite mechanisms. J. Mech. Mater. Struct. 2 (2), 293–301.

Hamermesh, M., 1962. Group Theory and its Application to Physical Problems. Pergamon Press, Oxford.

Harth, P., Michelberger, P., 2016. Determination of loads in quasi-symmetric structure with symmetry components. Eng. Struct. 123, 395–407.

Healey, T.J., Treacy, J.A., 1991. Exact block diagonalisation of large eigenvalue problems for structures with symmetry. Int. J. Numer. Methods Eng. 31, 265–285.

Healey, T.J., 1988. A group-theoretic approach to computational bifurcation problems with symmetry. Comput. Methods Appl. Mech. Eng. 67, 257–295.

Ikeda, K., Murota, K., 1991. Bifurcation analysis of symmetric structures using block--diagonalisation. Comput. Methods Appl. Mech. Eng. 86, 215–243.

Irvine, H.M., 1981. Cable Structures. MIT Press, Cambridge, MA.

Ivovich, V.A., Pokrovskii, L.N., 1991. In: Balkema, A.A. (Ed.), Dynamic Analysis of Suspended Roof Systems. Rotterdam.

Kangwai, R.D., Guest, S.D., 1999. Detection of finite mechanisms in symmetric structures. Int. J. Solids Struct. 36, 5507–5527.

Kangwai, R.D., Guest, S.D., 2000. Symmetry-adapted equilibrium matrices. Int. J. Solids Struct. 37, 1525–1548.

Kangwai, R.D., Guest, S.D., Pellegrino, S., 1999. An introduction to the analysis of symmetric structures. Comput. Struct. 71, 671–688.

Kaveh, A., Koohestani, K., 2008. Graph products for configuration processing of space structures. Comput. Struct. 86, 1219–1231.

Kaveh, A., Nikbakht, M., 2007. Decomposition of symmetric mass-spring vibrating systems using groups, graphs and linear algebra. Commun. Numer. Methods Eng. 23, 639–664.

Kaveh, A., Nikbakht, M., 2010. Improved group-theoretical method for eigenvalue problems of special symmetric structures using graph theory. Adv. Eng. Softw. 41, 22–31.

Kaveh, A., Rahami, H., 2004. An efficient method for decomposition of regular structures using graph products. Int. J. Numer. Methods Eng. 61 (11), 1797–1808.

Kaveh, A., Shojaei, I., 2015. Advances in swift analysis of structures: near-regular structures and optimal analysis and design. Adv. Eng. Softw. 90, 119–126.

Mohan, S.J., Pratap, R., 2004. A natural classification of vibration modes of polygonal ducts based on group theoretic analysis. J. Sound Vib. 269, 745–764.

Otto, F. (Ed.), 1966. Tensile Structures MIT Press, Cambridge, MA.

Pellegrino, S., Calladine, C.R., 1984. Two-step matrix analysis of prestressed cable nets. In: Proceedings of the Third International Conference on Space Structures, pp. 744–749.

Schonland, D., 1965. Molecular Symmetry. Van Nostrand, London.

Siev, A., 1963. A General Analysis of Prestressed Nets. Publications of the International Association for Bridge and Structural Engineering, vol. 23, pp. 283–292.

Suresh, K., Sirpotdar, A., 2006. Automated symmetry exploitation in engineering analysis. Eng. Comput. 21 (4), 304–311.

Szabo, J., Kollar, L., 1984. Structural Design of Cable-Suspended Roofs. Akademiai Kiado, Budapest.

Varkonyi, P.L., Domokos, G., 2007. Imperfect symmetry: a new approach to structural optima via group representation theory. Int. J. Solids Struct. 44 (14,15), 4723–4741.

Vilnay, O., Rogers, P., 1990. Statical and dynamical response of cable nets. Int. J. Solids Struct. 26, 299–312.

Vilnay, O., 1990. Cable Nets and Tensegric Shells. Ellis Horwood, Chichester.

Weyl, H., 1932. Theory of Groups and Quantum Mechanics. Dover Publications, New York.

Wigner, E.P., 1959. Group Theory and its Applications to the Quantum Mechanics of Atomic Spectra. Academic Press, New York.

Zingoni, A., Pavlovic, M.N., Zlokovic, G.M., 1995a. A symmetry-adapted flexibility approach for multi-storey space frames: general outline and symmetry-adapted redundants. Struct. Eng. Rev. 7, 107–119.

Zingoni, A., Pavlovic, M.N., Zlokovic, G.M., 1995b. A symmetry-adapted flexibility approach for multi-storey space frames: symmetry-adapted loads. Struct. Eng. Rev. 7, 121–130.

Zingoni, A., 1996. An efficient computational scheme for the vibration analysis of high-tension cable nets. J. Sound Vib. 189 (1), 55–79.

Zingoni, A., 1997. Shell Structures in Civil and Mechanical Engineering. Thomas Telford, London.

Zingoni, A., 2005. On the symmetries and vibration modes of layered space grids. Eng. Struct. 27 (4), 629–638.

Zingoni, A., 2008. On group-theoretic computation of natural frequencies for spring–mass dynamic systems with rectilinear motion. Commun. Numer. Methods Eng. 24, 973–987.

Zingoni, A., 2009. Group-theoretic exploitations of symmetry in computational solid and structural mechanics. Int. J. Numer. Methods Eng. 79, 253–289.

Zingoni, A., 2012a. A group-theoretic finite-difference formulation for plate eigenvalue problems. Comput. Struct. 112/113, 266–282.

Zingoni, A., 2012b. Symmetry recognition in group-theoretic computational schemes for complex structural systems. Comput. Struct. 94/95, 34–44.

Zingoni, A., 2014. Group-theoretic insights on the vibration of symmetric structures in engineering. Philos. Trans. R. Soc. A 372, 20120037.

Zingoni, A., 2015. Vibration Analysis and Structural Dynamics For Civil Engineers: Essentials and Group-Theoretic Formulations. CRC Press/Taylor and Francis, London.

Zlokovic, G.M., 1989. Group Theory and G-Vector Spaces in Structural Analysis. Ellis Horwood, Chichester.